nature astronomy

LETTERS

DOI: 10.1038/s41550-017-0269-z

Detection of nanoflare-heated plasma in the solar corona by the FOXSI-2 sounding rocket

Shin-nosuke Ishikawa[1*], Lindsay Glesener[2], Säm Krucker[3,4], Steven Christe[5], Juan Camilo Buitrago-Casas[3], Noriyuki Narukage[6] and Juliana Vievering[2]

The processes that heat the solar and stellar coronae to several million kelvins, compared with the much cooler photosphere (5,800 K for the Sun), are still not well known[1]. One proposed mechanism is heating via a large number of small, unresolved, impulsive heating events called nanoflares[2]. Each event would heat and cool quickly, and the average effect would be a broad range of temperatures including a small amount of extremely hot plasma. However, detecting these faint, hot traces in the presence of brighter, cooler emission is observationally challenging. Here we present hard X-ray data from the second flight of the Focusing Optics X-ray Solar Imager (FOXSI-2), which detected emission above 7 keV from an active region of the Sun with no obvious individual X-ray flare emission. Through differential emission measure computations, we ascribe this emission to plasma heated above 10 MK, providing evidence for the existence of solar nanoflares. The quantitative evaluation of the hot plasma strongly constrains the coronal heating models.

During an observation on 11 December 2014, the second flight of the Focusing Optics X-ray Solar Imager (FOXSI-2) sounding (research) rocket detected hard X-rays (HXRs, above ~3 keV in this article) from several active regions[3]. FOXSI is the first instrument to directly focus solar HXRs and achieve high-sensitivity imaging and spectroscopic observations[3–5]. Figure 1a shows a FOXSI-2 HXR image (cyan contours) of two such regions near disk centre overlaid on background soft X-ray (SXR, below ~3 keV) images taken by the X-ray Telescope (XRT) on-board the Hinode spacecraft. The XRT filter shown is sensitive to >2 MK plasma. Both northern and southern active regions (National Oceanic and Atmospheric Administration designations 12234 and 12230, respectively) showed HXR intensity changes at some point during the flight, but we were able to isolate a time with no significant HXR changes for active region 12234 (yellow box in Fig. 1a and blue box in Fig. 1b). We checked the SXR emissions detected by the Geostationary Operational Environmental Satellite (GOES) X-ray Sensor (XRS), which is typically used to identify flares. As can be seen in Fig. 1b, GOES/XRS observed no flare during the time interval shown in the blue box. SXRs and HXRs from active region 12234 (Hinode/XRT and FOXSI-2 lightcurves in Fig. 1b) in this time interval were constant within 1σ standard deviation uncertainties (indicated by the error bars in Fig. 1b). We thus conclude that active region 12234 was quiescent during this time interval. We define such a region a 'quiescent active region'. Despite the lack of distinct, resolved flares, FOXSI-2 successfully detected HXR emission up to 9 keV from the region.

The temperature structure of solar plasma can be evaluated by estimating the differential emission measure (DEM), which is the temperature-dependent brightness. Figure 2a shows the DEM of active region 12234, produced by combining HXR and SXR data for the time interval indicated in the blue box in Fig. 1b. (See Methods for details on the DEM computation.) Magenta curves in Fig. 2a are loci curves corresponding to observed values with individual XRT filter configurations using the latest calibration[6]. Blue loci curves show the detected HXR emissions by FOXSI-2 in three energy bands: 5–6 keV, 6–7 keV and 7–9 keV. Each curve indicates the amount of emission measure that would be needed to produce the observed intensity if the emitting plasma were isothermal at the temperature given in the abscissa. The true DEM distribution must lie below these loci curves. However, it must not lie too far below, because the total emission from the entire temperature distribution must produce the observed counts in each energy band. A precise DEM over a wide range of coronal temperatures was successfully obtained thanks to the combination of high-sensitivity SXR and HXR observations; the SXR emission determines the lower-temperature plasma, while HXRs indicate the presence of a faint, high-temperature component. The DEM value of this hot component at 10 MK is more than five orders of magnitude smaller than that at the peak of ~2.5 MK. This challenging dynamic range is successfully achieved by the combination of the different observational wavelength bands with a range of temperature sensitivities. Between the temperatures, T, of 4 MK and 10 MK, the DEM has approximately a steep power-law relation, $\propto T^{-12}$. The slope $\beta = 12$ is similar to the highest values for the upper power-law index of the distribution DEM $\propto T^{-\beta}$ in previous studies using extreme ultraviolet (EUV) line spectroscopy (β= 5–13 in ref. [7]). Figure 2b shows the HXR spectrum observed by FOXSI-2, overplotted with the spectrum predicted by the estimated DEM.

This hot plasma above 10 MK, although faint, is significant. The detected HXR counts above 7 keV (locus curve shown by the thick blue line in Fig. 2a) require the existence of hot (≥10 MK) plasma. The <10 MK plasma in this DEM distribution can account for only 7% or less of the counts detected in the 7–9 keV band. Even if we extend the power law at 4–10 MK to high temperatures, a total of only 10% of the detected 7–9 keV counts would be accounted for. We confirmed that the instrumental background is notably smaller than the detected intensity and that no detector pileup is expected (see Methods for details). This means that more than 90% of the

[1]Institute of Space and Astronautical Science, Japan Aerospace Exploration Agency, 3-1-1 Yoshinodai, Chuo-ku, Sagamihara, Kanagawa 252-5210, Japan. [2]School of Physics and Astronomy, University of Minnesota, Minneapolis, MN 55455, USA. [3]Space Sciences Laboratory, University of California, Berkeley, Berkeley, CA 94720, USA. [4]Institute of 4D Technologies, School of Engineering, University of Applied Sciences and Arts Northwestern Switzerland, 5210 Windisch, Switzerland. [5]NASA Goddard Space Flight Center, Greenbelt, MD 20771-0001, USA. [6]National Astronomical Observatory of Japan, 2-21-1 Osawa, Mitaka, Tokyo 181-8588, Japan. *e-mail: s.ishikawa@solar.isas.jaxa.jp

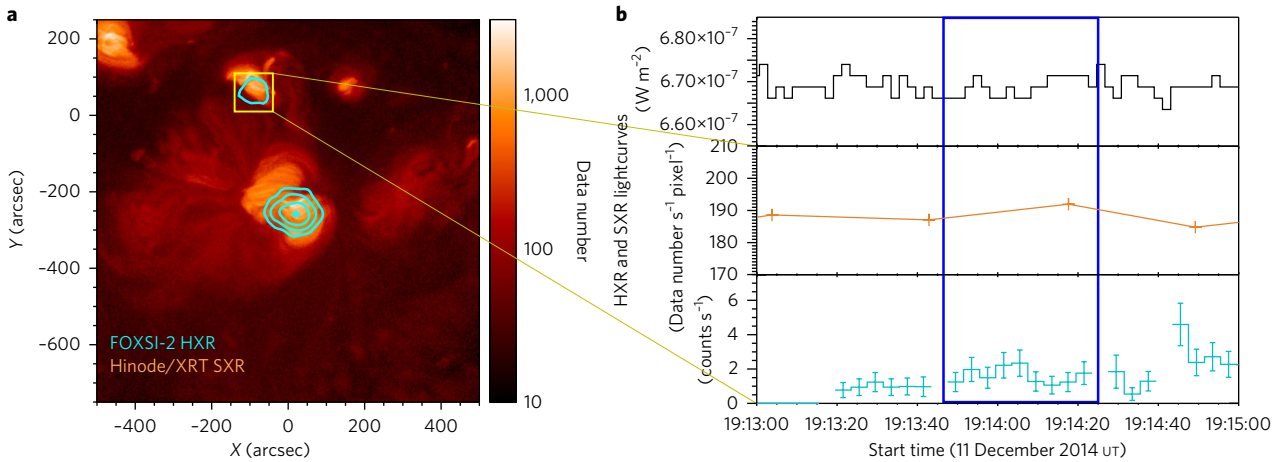

Fig. 1 | Image and lightcurves of the HXR and SXR emissions. a, HXR (above ~3 keV) emission observed by FOXSI-2 on 11 December 2014, 19:13:47–19:14:25 UT (cyan contours) overlaid on SXR (below ~3 keV) images (see colour scale) of two active regions taken with Hinode/XRT (sensitive to >2 MK). Active region 12234, shown in the yellow box, exhibited no individual flaring activity during the time interval, and was selected for the analysis. **b**, GOES/XRS (top), Hinode/XRT (middle) and FOXSI-2 (bottom) lightcurves. The GOES lightcurve is for the full Sun, and the XRT and FOXSI lightcurves are for 12234. The error bars in the FOXSI-2 lightcurve show 1σ standard deviation statistical errors. The gaps in the FOXSI-2 lightcurve show the intervals for pointing changes. The blue box shows the integration time for the FOXSI-2 image in **a**.

observed >7 keV HXR emissions must come from the ≥10 MK plasma, revealing a significant excess above the power-law DEM. The emission measure of the >10 MK plasma is in the range 1.8×10^{22}–1.5×10^{23} cm^{-5} in the solutions with chi-squared values within the 95% occurrence probability in trial runs (see Methods for details of the analysis). The >10 MK emission measure is >10^{22} cm^{-5} for 99.8% of the Monte Carlo solutions, and is >10^{21} cm^{-5} for all the solutions. Therefore, we conclude that significant HXRs from the >10 MK plasma component were detected.

Simulations show that nanoflare models can have temperatures beyond 10 MK (refs [8–10]). An alternative set of theories explains coronal heating via waves propagating from the photosphere to the corona, including shearing Alfvén waves[11]. However, it is difficult to produce plasma of 10 MK and above using wave heating models[12], and thus we interpret such a hot component to be an observational signature of frequent energy input by nanoflares[13]. Our observational result supplies quantified parameters (DEM power-law slope, quantity of >10 MK plasma) that will constrain future modelling of nanoflare distributions. Recently, a two-fluid simulation suggested that detectable >10 MK plasma could be generated only by short nanoflares with non-ionization equilibrium and an ignorable difference in ion and electron heating[14].

In past observations, the Reuven Ramaty High Energy Solar Spectroscopic Imager (RHESSI) detected HXRs from the Sun during periods with no flares by examining the day–night transitions of emission from the entire solar disk[15]. Those HXRs were from hot plasma with temperatures of 5–10 MK, and no >11 MK plasma was found. If we fit the FOXSI-2 spectrum with an isothermal model, the temperature of active region 12234 during the time period of this study is ~10 MK, towards the higher end of the range found for the Sun[15]. The emissions measure for 12234 is also more than three orders of magnitude smaller than the lowest emission measure detected by RHESSI from the non-flaring Sun. The fact that the temperature is within the range of the statistical study suggests that our target active region is not an exceptionally hot region.

This observation provides the most direct evidence to date for the presence of hot plasma in a quiescent solar active region. With the advent of directly focusing HXR instruments, we expect future observations to enable statistical studies and investigations of nanoflare-heated plasma and energy input to the corona. More high-sensitivity X-ray imaging and spectroscopic observations are expected with current and future instruments, including the next launch of FOXSI (FOXSI-3), the Nuclear Spectroscopic Telescope Array (NuSTAR) spacecraft[16] and a potential future solar-dedicated mission that is in the early stages of development.

Methods

Coronal DEMs are usually evaluated by EUV and SXR observations[7,17,18]. Because intensities of the EUV lines sensitive to high temperatures (~10 MK and above; for example, Fe XXIII and Fe XXIV lines with sensitivity peaks at 10–20 MK) are weak in the absence of large flares, only a few detections of those lines in quiescent active regions have been reported. The few positive reports[19] are based on multi-filter SXR observations by the XRT, especially using the thick filters. However, the XRT uncertainties are large in the temperature range of flare-heated plasma[20], and so the high-temperature components are poorly constrained without the additional use of bremsstrahlung HXRs. The primary solar HXR instrument is the RHESSI spacecraft, which has never detected significant emission localized in individual quiescent active regions due to limited sensitivity. In the case of ref. [19], follow-on work using RHESSI's non-detection was used to significantly constrain the hot plasma present[12]. In this case, RHESSI supplies only an upper limit, and the hot

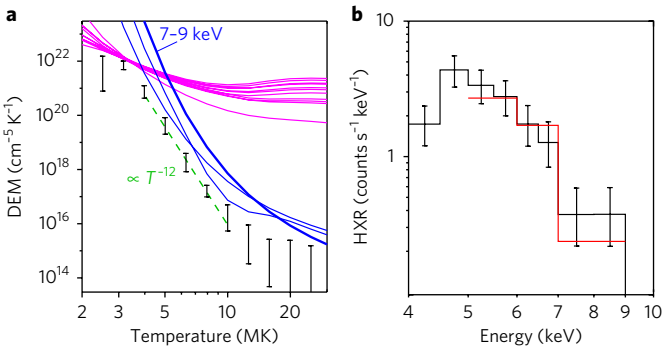

Fig. 2 | Estimated DEM and HXR spectrum of the quiescent active region. a, Estimated DEM of the quiescent active region from FOXSI-2 and Hinode/XRT observations, and loci curves for observed quantities. The error bars show a range of solutions with χ^2 values within the 95% occurrence probability in the Monte Carlo runs. Each curve corresponds to a filter configuration of Hinode/XRT (magenta) or a FOXSI-2 energy bin between 5 keV and 9 keV (blue). The thick blue curve indicates the 7–9 keV bin of FOXSI-2. **b**, HXR energy spectrum observed by FOXSI-2 (black), with the spectrum predicted by the estimated DEM (red). The error bars show 1σ statistical errors.

plasma could be constrained much more, or perhaps directly measured, with a lower-background, higher-sensitivity HXR instrument. HXR observations provide a more reliable method to investigate hot plasma than SXRs or EUV because the contributions of hot plasma and high-energy (non-thermal) electrons dominate this range. To investigate hot plasma in quiescent active regions using HXRs therefore requires the higher sensitivity that can be provided by newly available focusing optics that directly image HXRs.

FOXSI is a sounding rocket experiment to investigate HXR emissions in the 4–20 keV range from the Sun with superior sensitivity over previous, indirectly imaging, instruments[3,5]. The high sensitivity is achieved by a combination of directly focusing optics and semiconductor detectors for imaging and spectroscopy. Using a grazing incidence telescope with precision mirrors, we can increase effective area with a much smaller detector volume, drastically increasing the signal to background ratio and therefore the sensitivity. The first flight of FOXSI on 2 November 2012 successfully demonstrated the concept and effectivity of HXR focusing optics for solar observation by the observation of a microflare. FOXSI clearly showed greater sensitivity and imaging dynamic range than a simultaneous observation of the microflare by RHESSI[4]. During the same flight, FOXSI targeted a quiescent active region, but did not detect emission. This observation was used to constrain the hot plasma component of that active region[21]. On 11 December 2014, FOXSI-2 was flown for a 6.5 min observation at the White Sands Missile Range in New Mexico, United States, during which it successfully performed imaging and spectroscopy of multiple regions.

The FOXSI-2 instrument consists of seven optics modules, each paired with a dedicated semiconductor strip detector. The FOXSI optics are Wolter type-I grazing incidence telescopes developed at the NASA/Marshall Space Flight Center, with heritage from previous designs for non-solar astrophysics[22]. Multiple mirror shells (10 shells for two modules, and 7 shells for the other five) are nested together to increase collecting area. The optics are the highest-resolution HXR focusing optics ever used for astrophysics, with a measured spatial resolution of 5 arcsec (full-width at half-maximum) and a 27 arcsec half-power diameter[5].

The FOXSI-2 detectors are low-noise, fine-pitch, double-sided silicon (Si) and cadmium telluride (CdTe) detectors developed at the JAXA/Institute of Space and Astronautical Science by a team including development members of the Hard X-ray Imager and Soft Gamma-ray Detector on-board the Hitomi satellite. Spatial samplings are 75 μm and 60 μm, and measured energy resolutions are 0.5 keV and 1.3 keV (full-width at half-maximum) for the Si and CdTe detectors, respectively[23,24]. The sensitive areas are 9.6 mm × 9.6 mm and 7.68 mm × 7.68 mm for the Si and CdTe detectors, respectively, corresponding to respective fields of view of 16.5 arcmin × 16.5 arcmin and 13.2 arcmin × 13.2 arcmin. We newly developed the CdTe detectors for FOXSI-2 for higher efficiency for energies above 10 keV, and almost 100% efficiency was achieved for the FOXSI-2 energy range of 4–20 keV. We used five Si and two CdTe detectors for the FOXSI-2 flight. The FOXSI data consist of a list of detected photons with energies, incident locations and times. Images, lightcurves and energy spectra can be derived from this event list.

For FOXSI-2, we coordinated an observation of Hinode (Hinode Observation Plan 221). Our request to XRT included multi-filter images with a large field of view covering an area of 2,107 arcsec × 2,107 arcsec (more than the full solar disk size). XRT took images with 11 filter configurations, and it took ~6 min to take a full set. The region of interest in this study was outside the fields of view of the other Hinode instruments. In addition to the multi-filter observation, XRT took images with an identical filter configuration to check for flare occurrence, called the 'flare patrol' images. (The flare patrol can trigger a flare mode observation if a brightening is found, although none occurred during the FOXSI flight.) The XRT data in Fig. 1b are from flare patrol images.

We calculated the DEM by combining FOXSI-2 data integrated from 19:13:47 to 19:14:25 Universal Time (UT) and a single set of the XRT observations at 19:08:56–19:14:57 UT. We checked the flare patrol images and FOXSI lightcurves, and confirmed that the X-ray flux from this region was constant during this set of observations. The DEM calculation was performed in an area of 100 arcsec × 100 arcsec, centred at (−90 arcsec, 60 arcsec), shown in the yellow box in Fig. 1a, to cover the entire HXR emission detected by FOXSI-2. The DEM was estimated by a forward-fitting method to find the DEM solution to reproduce FOXSI-2 and XRT observations by assuming a smooth distribution represented by a spline function for the DEM curve. The procedure used in this work is xrt_dem_iterative2.pro, which is a standard tool set for solar data analysis in the Solar Software package. The details of this method are described in our previous paper[21]. We had 10,000 trial runs for the DEM estimation by varying each observational value randomly according to a Poisson distribution for the statistical error, and a range of solutions with chi-squared values within the 95% occurrence probability is shown in Fig. 2.

Although it is not statistically significant, a slight intensity increase in the FOXSI-2 lightcurve is seen at approximately 19:14:00 UT. We confirmed that the >7 keV HXRs were not concentrated at the time of the intensity increase, but instead were spread over the time range for the analysis. These photons are also not spatially concentrated at any preferred location within the active region. Therefore, we confirmed that the >7 keV emissions do not come predominantly from a single flaring event.

FOXSI-2 detected 15 photons within the 7–9 keV band from the region of interest during the time interval of this work, and no signal above 9 keV was detected. We examined, and ruled out, several other possibilities for the origin of these photons. The estimated background over the surrounding detector area is 0.9 ± 0.1 counts. This background includes non-solar charged particles, scattered photons from other solar sources (active region 12230 in Fig. 1) and any quiet Sun emission, if present. The background-subtracted measurement is $14 . 1^{+5}_{-4}$ counts, and this value was used for the DEM estimation. The expected 7–9 keV counts without the presence of the >10 MK plasma is 0.54 counts for the least chi-squared solution, meaning that the high-energy emission is not produced by the lower-temperature part of the DEM. We used the FOXSI-2 observation >5 keV because the uncertainty in the detection efficiency is greater at the lower detection limit energy of ~4 keV.

High energy counts could, in principle, be falsely recorded due to pileup of multiple incident photons. Pileup happens if two photons hit a single detector strip within a timescale of ~10 μs. The detector strip with the highest count rate from the target region has 1.0 counts per second in the 4–15 keV range during this pointing. Even if we assume the rate of the incident photons down to 3 keV is ten times more, the expected pileup count in this strip is 2.0×10^{-3} counts per second. By calculating the expected pileup counts for all the pixels assuming that there are ten times more incident ≥3 keV photons than the detected 4–15 keV counts for all the strips, the total expected pileup count by multiple ≥3 keV photons by all the detectors in this analysis is 0.33 counts. Therefore, the effect of pileup is negligible for the 7–9 keV counts, because the expected pileup count is well below the statistical error. After ruling out these alternative explanations for the high-energy emission, we can state with confidence that our detected photons are primarily due to >10 MK plasma in active region 12234.

Data availability. The data that support the plots within this paper and other findings of this study are available from the corresponding author upon reasonable request.

Received: 6 June 2017; Accepted: 1 September 2017;
Published online: 09 October 2017

References

1. Klimchuk, J. A. On solving the coronal heating problem. *Sol. Phys.* **234**, 41–77 (2006).
2. Parker, E. N. Nanoflares and the solar X-ray corona. *Astrophys. J.* **330**, 474–479 (1988).
3. Glesener, L., Krucker, S. & Christe, S. et al. The FOXSI solar sounding rocket campaigns. *Proc. SPIE* **9905**, 99050E (2016).
4. Krucker, S., Christe, S. & Glesener, L. et al. First images from the Focusing Optics X-Ray Solar Imager. *Astrophys. J.* **793**, L32 (2014).
5. Christe, S., Glesener, L. & Buitrago-Casas, C. et al. FOXSI-2: upgrades of the focusing optics X-ray solar imager for its second flight. *J. Astron. Instrum.* **5**, 1640005 (2016).
6. Narukage, N., Sakao, T. & Kano, R. et al. Coronal-temperature-diagnostic capability of the Hinode/X-Ray Telescope based on self-consistent calibration. II. Calibration with on-orbit data. *Sol. Phys.* **289**, 1029–1042 (2014).
7. Warren, H. P., Winebarger, A. R. & Brooks, D. H. A systematic survey of high-temperature emission in solar active regions. *Astrophys. J.* **759**, 141 (2012).
8. Cargill, P. J. & Klimchuk, J. A. Nanoflare heating of the corona revisited. *Astrophys. J.* **605**, 911–920 (2004).
9. Klimchuk, J. A., Patsourakos, S. & Cargill, P. J. Highly efficient modeling of dynamic coronal loops. *Astrophys. J.* **682**, 1351–1362 (2008).
10. Cargill, P. J., Bradshaw, S. J. & Klimchuk, J. A. Enthalpy-based thermal evolution of loops. II. Improvements to the model. *Astrophys. J.* **752**, 161 (2012).
11. Heyvaerts, J. & Priest, E. R. Coronal heating by phase-mixed shear Alfven waves. *Astron. Astrophys.* **117**, 220–234 (1983).
12. Schmelz, J. T., Kashyap, V. L. & Saar, S. H. et al. Some like it hot: coronal heating observations from Hinode X-ray Telescope and RHESSI. *Astrophys. J.* **704**, 863–869 (2009).
13. Klimchuk, J. A. Coronal loop models and those annoying observations! (Keynote). In *Proc. ASP Conference 'Second Hinode Science Meeting: Beyond Discovery-Toward Understanding'* 221–233 (Vol. 415, Astronomical Society of the Pacific, 2009).
14. Barnes, W. T., Cargill, P. J. & Bradshaw, S. J. Inference of heating properties from 'hot' non-flaring plasmas in active region cores. II. Nanoflare trains. *Astrophys. J.* **833**, 217 (2016).
15. McTiernan, J. M. RHESSI/GOES observations of the nonflaring Sun from 2002 to 2006. *Astrophys. J.* **697**, 94–99 (2009).
16. Hannah, I. G., Grefenstette, B. W. & Smith, D. M. et al. The first X-ray imaging spectroscopy of quiescent solar active regions with NuSTAR. *Astrophys. J.* **820**, L14 (2016).
17. Winebarger, A. R., Schmelz, J. T., Warren, H. P., Saar, S. H. & Kashyap, V. L. Using a differential emission measure and density measurements in an active region core to test a steady heating model. *Astrophys. J.* **740**, 2 (2011).

18. Aschwanden, M. J. & Boerner, P. Solar corona loop studies with the Atmospheric Imaging Assembly. I. Cross-sectional temperature structure. *Astrophys. J.* **732**, 81 (2011).
19. Schmelz, J. T., Saar, S. H. & DeLuca, E. E. et al. Hinode X-Ray Telescope detection of hot emission from quiescent active regions: a nanoflare signature? *Astrophys. J.* **693**, L131–L135 (2009).
20. Winebarger, A. R., Warren, H. P. & Schmelz, J. T. et al. Defining the 'blind spot' of Hinode EIS and XRT temperature measurements. *Astrophys. J.* **746**, L17 (2012).
21. Ishikawa, S., Glesener, L. & Christe, S. et al. Constraining hot plasma in a non-flaring solar active region with FOXSI hard X-ray observations. *Publ. Astron. Soc. Jpn* **66**, S15 (2014).
22. Ramsey, B. D. The development of focusing optics for the hard-X-ray region. *Adv. Space Res.* **38**, 2985–2988 (2006).
23. Ishikawa, S., Saito, S. & Tajima, H. et al. Fine-pitch semiconductor detector for the FOXSI mission. *IEEE T. Nucl. Sci.* **58**, 2039–2046 (2011).
24. Ishikawa, S., Katsuragawa, M. & Watanabe, S. et al. Fine-pitch CdTe detector for hard X-ray imaging and spectroscopy of the Sun with the FOXSI rocket experiment. *J. Geophys. Res. Space Phys.* **121**, 6009–6016 (2016).

Acknowledgements

We acknowledge the FOXSI instrument team for the development of the experiment. The X-ray focusing optics were provided by a team at NASA/Marshall Space Flight Center led by B. Ramsey. The focal plane detectors were developed by a team at ISAS/JAXA led by T. Takahashi and S. Watanabe. This work was supported through KAKENHI grants 24244021 and 20244017 from the Japan Society for the Promotion of Science. FOXSI was funded by NASA's Low-Cost Access to Space program, grant NNX11AB75G. L.G. is supported by an NSF grant (AGS-1429512). Hinode is a Japanese mission developed and launched by ISAS/JAXA, with NAOJ as domestic partner and NASA and STFC (UK) as international partners. It is operated by these agencies in cooperation with ESA and NSC (Norway). The FOXSI team thanks NASA's Sounding Rockets Program Office and the NSROC teams who helped to attain a successful flight.

Author contributions

S.I., L.G., S.K., S.C. and J.B. contributed to the instrument development, analysis of the observational data, scientific discussions and text writing. N.N. contributed to the analysis of the data observed by the Hinode satellite and scientific discussions. J.V. contributed to software developments for the FOXSI data analysis.

Competing interests

The authors declare no competing financial interests.

Additional information

Reprints and permissions information is available at www.nature.com/reprints.

Correspondence and requests for materials should be addressed to S.-n.I.

Publisher's note: Springer Nature remains neutral with regard to jurisdictional claims in published maps and institutional affiliations.